COMPUTATION OF SMOKE SPREAD IN A BUILDING FIRE BY MULTI-LAYER ZONE MODEL

K. Suzuki
Institute of Technology, Shimizu Construction Corporation
3-4-17 Etchujima Koto-ku, Tokyo 135-8530, Japan

T. Tanaka
Disaster Prevention Research Institute, Kyoto University, Gokasho, Uji, Kyoto 611-0011, Japan

K. Harada
Department of Architecture and Architectural Engineering, Graduate School of Engineering
Kyoto University, Katsura Campus C2-406, Nishikyo-ku, Kyoto 615-8540, Japan

ABSTRACT

The multi-layer zone fire smoke movement simulation model (called as MLZ model), a new zone modeling approach, was addressed to predict vertical distributions of the physical properties, such as temperature and chemical species concentration in a building fire. The model still retains the advantage of other zone models in terms of light computational load, so it is expected to be useful for a practical application for fire safety design of a building. In this study, the verification against a fire experiment in a multi-room area is presented. As the result, the predicted temperatures and gas velocity generally show satisfactory agreement. Additionally, a GUI tool which decreases the user's load for calculation settings and which displays calculation results by color on a two-dimensional plane was introduced.

KEYWORDS: Multi-layer zone model, Smoke movement, Fire experiment, GUI tool

INTRODUCTION

A multi-layer zone model, a new zone modeling approach, was applied to predict vertical distributions of the physical properties in a building fire. As illustrated in Fig. 1, the space volume of each room is divided into an arbitrary number of multiple layers as the control volumes in which the physical properties are assumed to be uniform. The boundary walls are also divided into segments in accordance with the layer divisions, and the convection and radiation heat transfer among the layers and the wall segments are calculated. In this way, the vertical distributions of the physical properties in each room are calculated. However the model still retains the advantage of two-layer zone models, such as CFAST and BRI2002 [1], in terms of light computational load, so it is expected to be useful for a practical application for fire safety design of buildings.

These basic concepts of the MLZ model for a single room and for a tunnel were introduced [2,3]. In this study, the model is extended to a multi-room configuration and improvements are made on the influence of ventilation flow to fire plume, the prediction of the ceiling jet, the entrainment of the opening jet plume and the radiation heat transfer from the flame. The results of the validation against a fire experiment in a building are demonstrated.

THE MODEL

The image of the fluid movement in the MLZ model is demonstrated in Fig. 1. One of the notable differences of the concept from the existing two-layer zone models is that the fire plume flow does not mix with the upper layer the instant it penetrates the layer interface but continues to rise until it hits the

1

ceiling, after which it pushes down the gases in the top layer while flowing horizontally as a ceiling jet. The image of temperature prediction in a fire room by the MLZ model relative to that by a two-layer zone model is on the left side of Fig. 1. The two-layer zone model predicts the layer interface height and only two temperature values, i.e. those of upper and lower layers. In the case of the MLZ model, the distribution of temperature can be predicted by calculating the temperatures of the multiple layers of which positions are arbitrarily pre-fixed.

(1) Governing Equation for Zone Properties
The zone governing equation for the temperature of each layer is derived from the conservation equations of mass and internal energy for each horizontal layer as follows:

$$\frac{dT_{i,j}}{dt} = \frac{1}{C_p \rho_{i,j} V_{i,j}} \Big[h_{i,j+1} - h_{i,j} - C_p m_{l,i,j+1} T_{i,j} + C_p m_{l,i,j} T_{i,j} + h_{op,i,j} + h_{fp,i,j} + Q_{cw,i,j} + Q_{rl,i,j} \Big] \quad [1]$$

$$h_{i,j} = \begin{cases} C_p m_{l,i,j} T_{i,j} & (m_{l,i,j} \ge 0) \\ C_p m_{l,i,j} T_{i,j-1} & (m_{l,i,j} < 0) \end{cases} \quad [2]$$

where $m_{l,i,j}$ and $h_{i,j}$ are the vertical mass and enthalpy flow rate through the boundary between the jth layer and the $(j+1)^{th}$ layer outside of the fire plume, respectively. $Q_{cw,i,j}$ is the convection heat gain from wall and $Q_{rl,i,j}$ is the net radiation heat gain. Subscript i means room i. The enthalpy of the fire plume, $h_{fp,i,j}$, is added only when entering the top layer of the fire room, and in the other layer it equals zero. The enthalpies of ventilation flow are transferred to the ceiling or floor by buoyancy through the opening jet plume, then the enthalpy of it, $h_{op,i,j}$, is added only to the layer in which opening jet plume reached.

Likewise, the zone governing equations for mass fraction of species l (i.e. CO_2) in each layer can be derived.
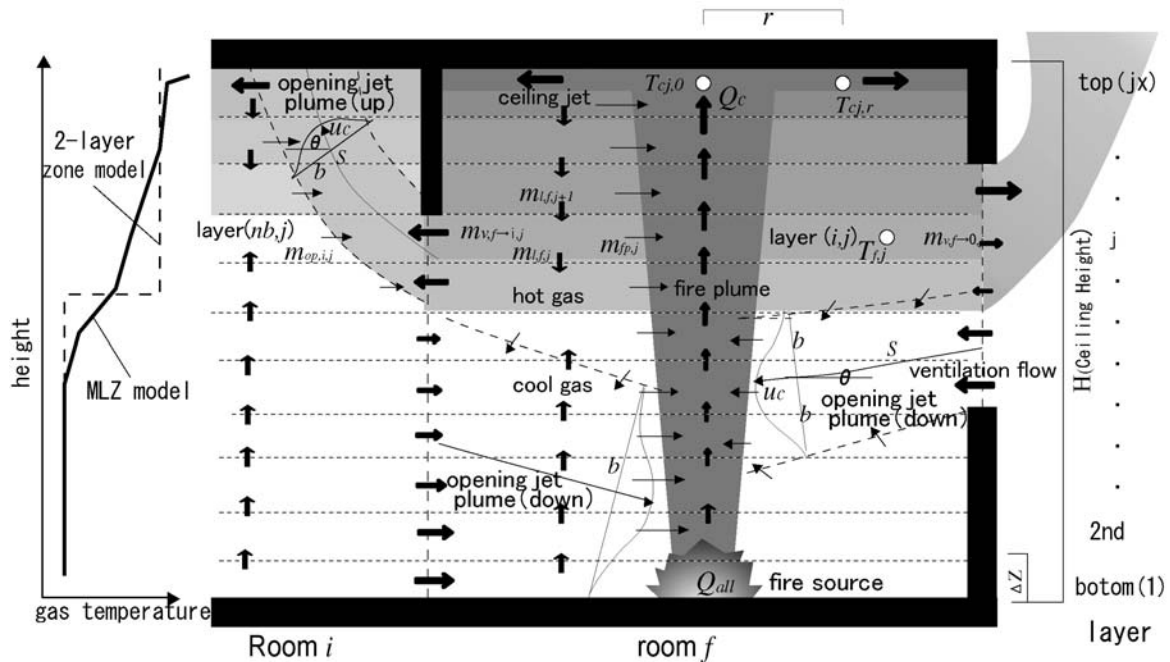
FIGURE 1. Image of MLZ model (a graph of left side shows comparison with temperature prediction image of MLZ and 2-layer zone)

(2) Flow through the Openings

Summing up the energy conservation equations in each room of the atmospheric pressure, the following equation could be written,

$$C_p \left(\sum_{nb} \sum_{j=1}^{jx} m_{nb \to i,j} T_{nb,j} - \sum_{nb} \sum_{j=1}^{jx} m_{i \to nb,j} T_{i,j} \right) + \sum_{j=1}^{jx} Q_{cw,i,j} + \sum_{j=1}^{jx} Q_{rl,i,j} + Q_c = 0 \qquad [3]$$

where Q_c, the convective heat from the fire source, which equals zero except for in the fire room. The horizontal mass flow rates through the openings, $m_{i \to nb,j}$ and $m_{nb \to i,j}$, are calculated from Eq. [4] and Eq. [5].

$$\begin{cases} m_{i \to nb,j} = \alpha_v B_{i \to nb,j} \Delta z \sqrt{2\rho_{i,j} \left(P_{i,j} - P_{nb,j} \right)} & \left(P_{i,j} - P_{nb,j} \geq 0 \right) \\ m_{nb \to i,j} = \alpha_v B_{i \to nb,j} \Delta z \sqrt{2\rho_{nb,j} \left(P_{nb,j} - P_{i,j} \right)} & \left(P_{i,j} - P_{nb,j} < 0 \right) \end{cases} \qquad [4]$$

$$P_{i,j} = P_{i,0} - g \sum_{k=1}^{j} \rho_{i,k} \Delta z \qquad [5]$$

Here, Eq. [3] can be solved for the value of the pressure of room i at the floor height, $P_{i,0}$, by an appropriate iteration method, because it includes $P_{i,0}$ implicitly, i.e. starting from an initial value of $P_{i,0}$ and calculating $m_{i \to nb,j}$ and $m_{nb \to i,j}$ by Eq. [4], next substituting them into the left hand side of Eq. [3], then modifying $P_{i,0}$ iteratively until the value of the left hand side of Eq. [3] becomes close enough to zero. This process is repeated to all rooms by the Gauss-Seidel method, thus $P_{i,0}$ of all rooms and horizontal mass flow rates are calculated implicitly.

The flows that have passed through openings become opening jet plumes by buoyancy. They change direction upward or downward, depending on their temperature relative to the environment, entraining the gas around it. The temperature, the velocity, the half-width and the trace of the axis are calculated by arranging the conservation equations of mass, energy, and moment for two-direction.

(3) Fire Plume Entrainment

The mass entrainment rate into the fire plume from the jth layer, $m_{fp,j}$, and the enthalpy transported through fire plume into the top layer, h_{fp}, are assumed to be given [4]:

$$m_{fp,j} = C_{e,j} Q_c^{1/3} \left(z_j^{5/3} - z_{j-1}^{5/3} \right) \qquad [6]$$

where the entrainment coefficient of fire plume, $C_{e,j}$, is estimated as 0.08 in the windless condition, while the value increases by the influence of the draft from the openings on the fire plume. The plots in Fig. 2 shows the relation of the ratio of $m_{fp,j}$ divided by the entrained mass flow rate in windless condition, $m_{fp,j}^0$, and the ratio of the ventilation velocity, U_j, divided by the velocity of the fuel, $w*$ [5]. Thus in this study, shown as the thick line in Fig. 2, it is assumed to have a linear relation in $0.0833 \leq U_j / W^* \leq 0.25$ as follows:

$$\frac{m_{fp,j}}{m_{fp,j}^0} = 8.33 \frac{U_j}{w^*} \qquad [7]$$

$$w^* = \frac{Q_c g}{0.5 D \rho T C_p} \tag{8}$$

From Eqs. [6], [7] and [8], the equation for $C_{e,j}$ is given as $0.08 \times 12 U_j / W^*$. When U_j is too high, $U_j / W^* > 0.25$, or U_j is too low, $U_j / W^* < 0.0833$, then $C_{e,j}$ is decided as 0.24 and 0.08, respectively.

$$C_{e,j} = \begin{cases} 0.08 \times 3 & \left(12 \dfrac{U_j}{W^*} \geq 3\right) \\[2mm] 0.08 \times 12 \dfrac{U_j}{W^*} & \left(1 < 12 \dfrac{U_j}{W^*} < 3\right) \\[2mm] 0.08 \times 1 & \left(12 \dfrac{U_j}{W^*} \leq 1\right) \end{cases} \tag{9}$$
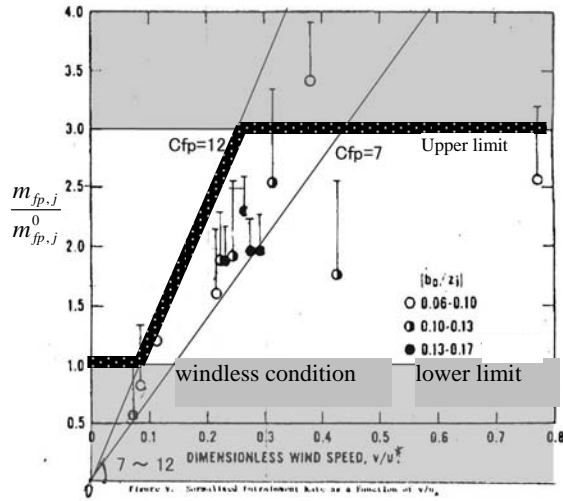
FIGURE 2. Relation of horizontal flow and entrainment increase rate

(4) Temperature of Ceiling Jet

The temperature rise of ceiling jet under an unconfined ceiling under calm conditions, $\Delta T_{cj,0}^{FC}$ and $\Delta T_{cj,r}^{FC}$, can be calculated by the following equations [6]:

$$\Delta T_{cj,0}^{FC} \equiv T_{cj,0}^{FC} - T_\infty = 16.9 \left(\frac{Q^{2/3}}{H^{5/3}} \right) \qquad \left(\frac{r}{H} \leq 0.18 \right) \tag{10}$$

$$\Delta T_{cj,r}^{FC} \equiv T_{cj,r}^{FC} - T_\infty = 5.38 \left(\frac{Q^{2/3}}{H^{5/3}} \right) \left(\frac{r}{H} \right)^{-2/3} \qquad \left(0.18 < \frac{r}{H} \right) \tag{11}$$

To apply Eqs. [10] and [11] to a fire in a compartment with a confined ceiling, consideration should be made of the following issues: a) the entrainment of a fire plume increases by the draft from openings as discussed in section (2), b) the enthalpy of the fire plume increases due to the entrainment of the hotter gas from the layers at elevated temperature and c) the enthalpy into the ceiling jet increases by

4

the same reason. Hence, the calculation method for the temperature rise of ceiling jet in a compartment fire, $\Delta T_{cj,0}$ and $\Delta T_{cj,r}$, is introduced as follows:

a) Increase of the fire plume entrainment by draft

The temperature rise of ceiling jet adapted for the increase of the mass flow rate from $m_{fp,j}^0$ to $m_{fp,j}$ by draft, $\Delta T_{cj,0}^{FC'}$ and $\Delta T_{cj,r}^{FC'}$, can be obtained as follows: letting the adjusted ceiling height, or entrainment height H' be:

$$H' = \left(\sum_{j=1}^{jx} m_{fp,j} \Big/ \sum_{j=1}^{jx} m_{fp,j}^0 \right)^{3/5} H \tag{12}$$

Substituting H' for H in Eqs. [10] and [11] yields:

$$\Delta T_{cj,0}^{FC'} = 16.9 \left(\frac{Q^{2/3}}{H'^{5/3}} \right) \qquad \left(\frac{r}{H'} \leq 0.18 \right) \tag{13}$$

$$\Delta T_{cj,r}^{FC'} = 5.38 \left(\frac{Q^{2/3}}{H'^{5/3}} \right) \left(\frac{r}{H'} \right)^{-2/3} \qquad \left(0.18 < \frac{r}{H'} \right) \tag{14}$$

b) Influence of plume entrainment from layers at elevated temperature into the fire plume

From the energy conservation of the fire plume, $\Delta T_{cj,0}$ is calculated as:

$$\Delta T_{cj,0} = \Delta T_{cj,0}^{FC'} + \frac{\displaystyle\sum_{j=1}^{jx} m_{fp,j} \left(T_{f,j} - T_\infty \right)}{\displaystyle\sum_{j=1}^{jx} m_{fp,j}} \qquad \left(\frac{r}{H'} \leq 0.18 \right) \tag{15}$$

c) Influence of hot gas entrained into the ceiling jet

Considering the energy conservation for the ceiling jet under unconfined ceiling without wind, the mass flow rate entrained by the ceiling jet at radial distance r from the impinging point, $m_{cj,r}$, is found to be:

$$m_{cj,r} = \left(\frac{\Delta T_{cj,0}^{FC}}{\Delta T_{cj,r}^{FC}} - 1 \right) \sum_{j=1}^{jx} m_{fp,j} = \left\{ 3.14 \left(\frac{r}{H'} \right)^{2/3} - 1 \right\} \sum_{j=1}^{jx} m_{fp,j} \tag{16}$$

Assuming that $m_{cj,r}$ can be obtained by Eq. [16] in an unconfined ceiling configuration, the equation for $\Delta T_{cj,r}$ is obtained by combining the energy conservation of the ceiling jet and Eq. [16] as follows:

$$\Delta T_{cj,r} = \Delta T_{cj,r}^{FC'} + \frac{\sum_{j=1}^{jx} m_{fp,j}\left(T_{f,j} - T_{\infty}\right)}{\sum_{j=1}^{jx} m_{fp,j} + m_{cj,r}} + \frac{m_{cj,r}\left(T_{f,jx} - T_{\infty}\right)}{\sum_{j=1}^{jx} m_{fp,j} + m_{cj,r}} \quad \left(\frac{r}{H'} > 0.18\right) \tag{17}$$

(5) Radiation Heat Transfer
In the model, the radiation heat flux is assumed to consist of three directional components between layers or layer and wall, i.e. the upward, the downward and the horizontal one from each layer. The upward, downward and horizontal heat fluxes, $\dot{q}_{ru,i,j}$, $\dot{q}_{rd,i,j}$ and $\dot{q}_{rw,i,j}$ are calculated as follows:

$$\dot{q}_{ru,i,j} = \left(1 - \alpha_{g,i,j}\right)F_{LU,i,j}\dot{q}_{ru,i,j-1} + \alpha_{g,i,j}\sigma T_{i,j}^4 + \left(1 - \alpha_{g,i,j}\right)F_{WU,i,j}\left\{\left(1 - \alpha_{w,i,j}\right)\dot{q}_{rw,i,j} + \alpha_{w,i,j}\sigma T_{ws,i,j}^4\right\} \tag{18}$$

$$\dot{q}_{rd,i,j} = \left(1 - \alpha_{g,i,j}\right)F_{UL,i,j}\dot{q}_{rd,i,j+1} + \alpha_{g,i,j}\sigma T_{i,j}^4 + \left(1 - \alpha_{g,i,j}\right)F_{WL,i,j}\left\{\left(1 - \alpha_{w,i,j}\right)\dot{q}_{rw,i,j} + \alpha_{w,i,j}\sigma T_{ws,i,j}^4\right\} \tag{19}$$

$$\dot{q}_{rw,i,j} = \left(1 - \alpha_{g,i,j}\right)\left(F_{LW,i,j}\dot{q}_{ru,i,j-1} + F_{UW,i,j}\dot{q}_{rd,i,j+1}\right) + \alpha_{g,i,j}\sigma T_{i,j}^4 + Q_{rfw,j}/A_{w,i,j} \tag{20}$$

where $\alpha_{w,i,j}$ are the radiation absorptivity, which is the same as the emissivity, of the wall surface. Only in the fire room, radiation from the flame of the fire source to walls, partially absorbed in layers, is considered, as shown as broken lines in Fig. 3. The fraction of radiation heat from the flame directing to the surface of the jth wall segment, $Q_{rf,j}$, is given as:

$$Q_{rf,j} = Q_r F_{FW,j} \tag{21}$$

where Q_r is the radiation heat emitted from the fire source and $F_{FW,j}$ is the ratio of radiation heat from the fire source directing to the jth wall. The fraction of $Q_{rf,j}$ reached j^{th}, $Q_{rfw,j}$, is calculated by Eq. [22,] subtracted the radiation heat absorbed by the layers (1st - j^{th}) from $Q_{rf,j}$:

$$Q_{rfw,j} = \left(1 - \alpha_{g,f,j}\right)\left(1 - \alpha_{g,f,j-1}\right)\cdots\left(1 - \alpha_{g,f,1}\right)Q_{rf,j} \tag{22}$$

where $\alpha_{g,i,j}$, the radiation absorptivity of the jth layer of the ith room, changes according to the gas temperature and mass fractions of CO_2, H_2O and soot, of which the spectra are not uniform. In this model, the Fortran program ABSORB, developed by Modak [7], is used to calculate $\alpha_{g,i,j}$. In the other hand, the total radiation absorbed in the jth layer from the fire point,

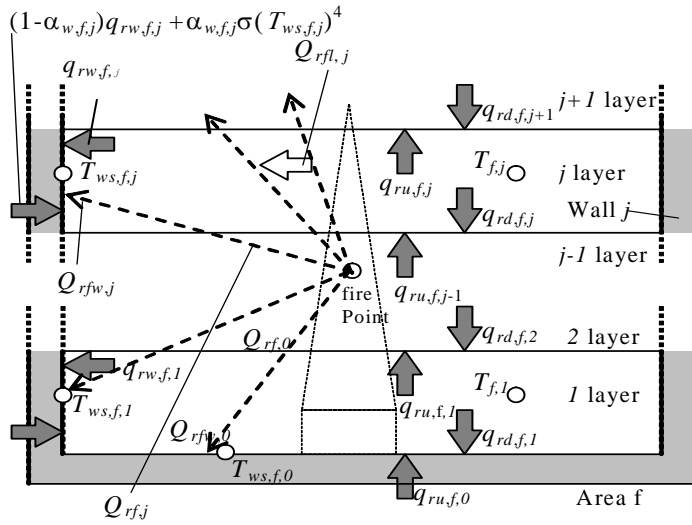$$Q_{rfl,j} = \sum_{k=j}^{jx} \alpha_{f,j}\left(1 - \alpha_{f,j-1}\right)\cdots\left(1 - \alpha_{f,1}\right)Q_{rf,k} \tag{23}$$

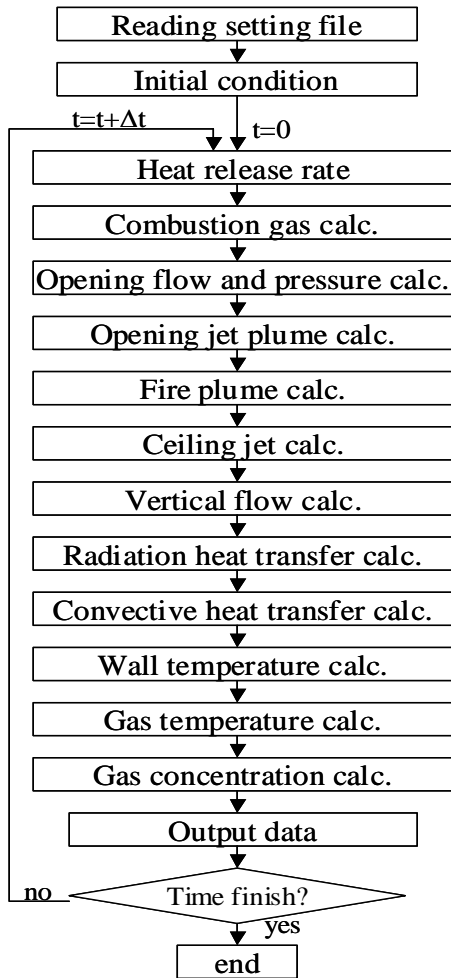Thus the net radiation heat gain of the jth layer of the ith room, $Q_{rl,i,j}$, is:

$$\begin{aligned}
Q_{rl,i,j} = {} & A_{f,i,j}\left(\dot{q}_{ru,i,j-1} - \dot{q}_{rd,i,j}\right) + A_{f,i,j+1}\left(-\dot{q}_{ru,i,j} + \dot{q}_{rd,i,j+1}\right) \\
& + A_{w,i,j}\left[\dot{q}_{rw,i,j} - \left\{\left(1 - \alpha_{w,i,j}\right)\dot{q}_{rw,i,j} + \alpha_{w,i,j}\sigma T_{w,i,j}^4\right\}\right] + Q_{rfl,j}
\end{aligned} \tag{24}$$

(6) Calculation Flow

Fig. 4 shows the flow chart of this model.

$$(1-\alpha_{w,f,j})q_{rw,f,j} + \alpha_{w,f,j}\sigma(T_{ws,f,j})^4$$

FIGURE 3. Image of radiation transfer in fire room

```
┌──────────────────────────┐
│   Reading setting file    │
└──────────────────────────┘
              ↓
┌──────────────────────────┐
│     Initial condition     │
└──────────────────────────┘
 t=t+Δt        ↓    t=0
┌──────────────────────────┐
│     Heat release rate     │
└──────────────────────────┘
              ↓
┌──────────────────────────┐
│   Combustion gas calc.    │
└──────────────────────────┘
              ↓
┌──────────────────────────────┐
│ Opening flow and pressure calc.│
└──────────────────────────────┘
              ↓
┌──────────────────────────┐
│  Opening jet plume calc.  │
└──────────────────────────┘
              ↓
┌──────────────────────────┐
│     Fire plume calc.      │
└──────────────────────────┘
              ↓
┌──────────────────────────┐
│     Ceiling jet calc.     │
└──────────────────────────┘
              ↓
┌──────────────────────────┐
│     Vertical flow calc.   │
└──────────────────────────┘
              ↓
┌──────────────────────────┐
│ Radiation heat transfer calc.│
└──────────────────────────┘
              ↓
┌──────────────────────────┐
│ Convective heat transfer calc.│
└──────────────────────────┘
              ↓
┌──────────────────────────┐
│   Wall temperature calc.  │
└──────────────────────────┘
              ↓
┌──────────────────────────┐
│   Gas temperature calc.   │
└──────────────────────────┘
              ↓
┌──────────────────────────┐
│  Gas concentration calc.  │
└──────────────────────────┘
              ↓
┌──────────────────────────┐
│        Output data        │
└──────────────────────────┘
              ↓
no  ◇─── Time finish? ───◇
              ↓ yes
┌──────────┐
│   end    │
└──────────┘
```

FIGURE 4. Flow chart

COMPARISON WITH EXPERIMENTAL RESULTS

(1) Experimental Data
In this section, the results of temperature and velocity measurements in 4 cases of the fire experiments are compared with the predictions by the model for validation. The experimental setup of the room of the fire origin, the plane of the whole experimental structure layout and a picture of the fire room are shown in Figs. 5, 6 and 7, respectively. The experimental fields, adjusted by the openings, and the fire source conditions are shown in Table 1. The total heat release rate data of the fire sources was obtained by measuring the weight loss of the fuel (n-Heptane) and multiplying the heat of combustion per unit fuel (44.4 MJ/kg), as shown in Fig. 8. The vertical distributions of gas and wall surface temperature were measured by thermocouples and the velocity distributions at the openings were measured by Pitot tubes and differential pressure gauges. As the ceiling jet, the temperature at the point 20 mm below the ceiling at 2 m distance from the center of the fire source was measured by thermocouple.
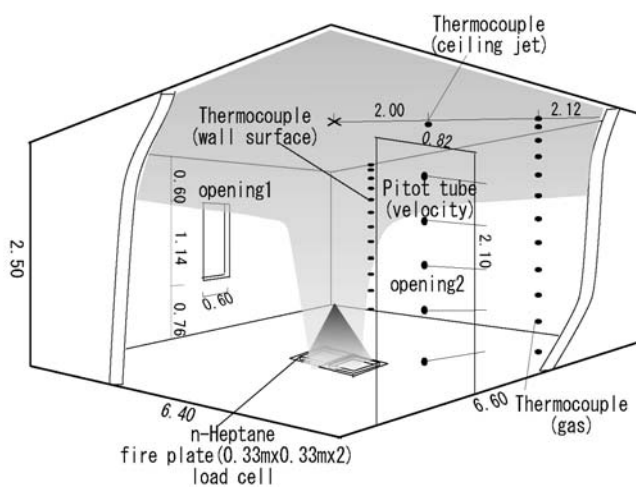
FIGURE 5. Schematic of fire room
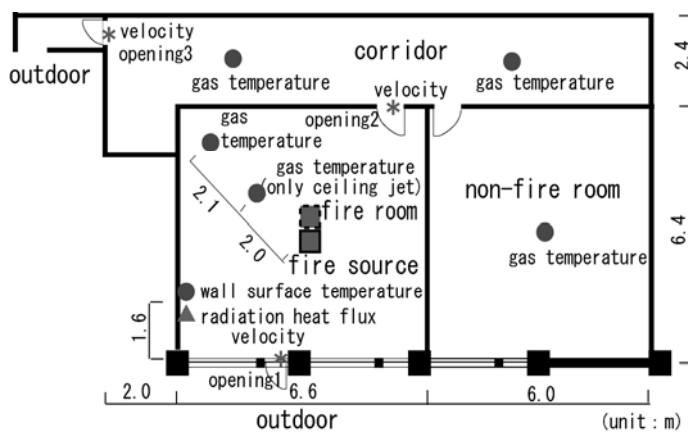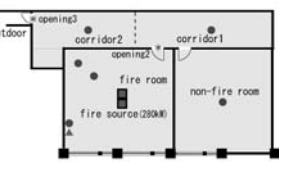

FIGURE 6. Plane of experiment field
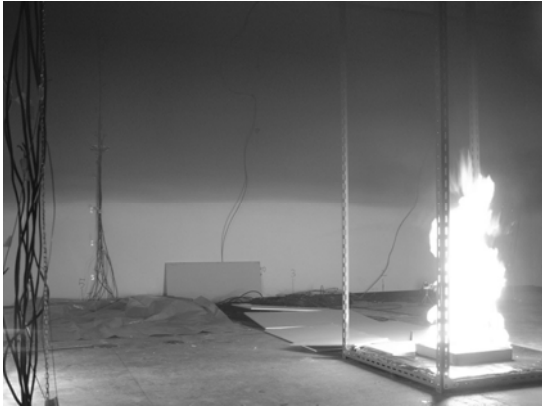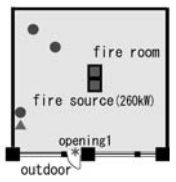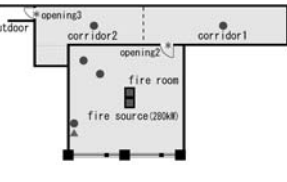
FIGURE 7. A picture of fire room
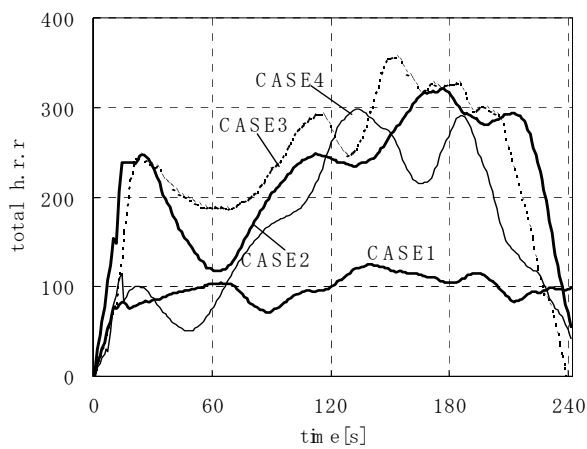
FIGURE 8. Total heat release rate

TABLE 1. Summary of experimental conditions (4 cases)

	Case 1	Case 2	Case 3	Case 4
domain	fire room	fire room	fire room+ corridor	fire room+corridor
opening (height-width[m])	opening1 (0.6x1.14)	opening1 (0.6x1.14)	opening2(2.1x0.8) opening3(2.0x0.8)	opening2(2.1x0.8) opening3(2.0x0.8) opening4(2.1x0.8)
Firepan (area)	1pan (0.11 m^2)	2 pans (0.22 m^2)	2 pans (0.22 m^2)	2 pans (0.22 m^2)
peak H.H.R.	120 kW	320 kW	350 kW	300 kW

(2) Condition of the Calculation
The calculation domain consists of 4 spaces, i.e., the two rooms and the corridor that is virtually divided into two at the center for better precision of the prediction. Each space is divided into 12 horizontal layers of equal thickness. The conditions, such as the areas of rooms, the ceiling height, the

initial air temperature and the total heat release rate were determined basically according to the experimental conditions for each case. In the experiment, most of the partition walls were assembly walls with 24 mm plaster board on both sides and 50 mm glass wool in between. However, in the calculation the walls were simplified as 48 mm plaster boards. The property of the ceiling and the floor were set as 12 mm plaster board and 100 mm concrete according to the conditions of the experiment. The calculation time step was 1 s. The flow coefficient, α_v, was set to 0.7 on the openings and 0.95 on the virtual boundary of the center of the corridor.

(3) Computer Load
The CPU time of the calculation for each case was within 30 s for computing 240 s by a PC with Pentium4 2.4 GHz, hence it could be found that this model has the advantage of computing load.

(4) Results and Discussion
Fig. 9 shows the comparison between the experiments and the calculations of the vertical distribution of the temperature in the fire room, the corridor (case 3 and 4 only) and the non-fire room (case 4 only) at 60, 120 and 180 s. The calculations in the fire room generally show satisfactory agreement with the experiments. However, they were a little lower at 0.3 to 1.2 m from the floor, and especially at 60 s in case 4 the calculation was fairly lower. The main reasons are suspected to be that the total heat release rate measured in the experiment might not be so accurate and that the experiments are influenced by radiation heat of the flame. The calculations in the corridor were higher at 0.9 to 1.4 m from the floor in case 3 and at 1.2 to 1.4 m from the floor in case 4, because the influence of the diffusion and the entrainment into the opening jet might be calculated less.

Fig. 10 shows the comparison with the temperature on the wall surface in the fire room and the same conclusion can be found with Fig. 9.
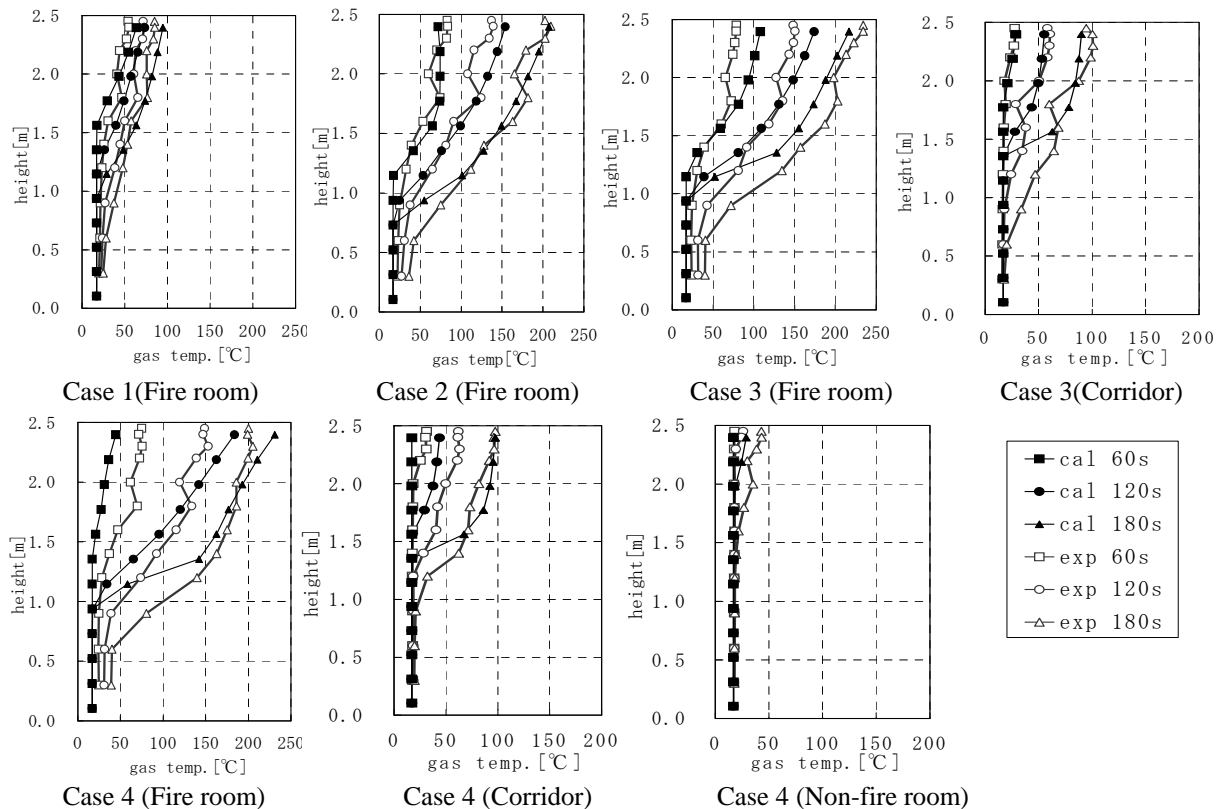
FIGURE 9. Gas temperature in fire room, corridor and non-fire room

Fig. 11 shows the comparison of the temperatures measured under the ceiling and the ceiling jet temperature predicted by Eq. [17], and for reference by Eq. [15] (r = 0) and Eq. [11] (r = 2, original Alpert's equation). Within 60 s in case 1 to 3, the calculations were high. The reason is unclear, but Eq. [11] was tuned for steady condition, hence the applicability might be beyond the range for the quick increase of the heat release. In the other, the comparisons were slightly high.

Fig. 12 shows the comparison with the velocity through the opening. The calculations were roughly coincident with the experiments, but some of the neutral heights were different. It seems that the experiments were measured only along the centerline of the opening so they were different with the average value of the opening area. The influence of entering wind from outside could also be considered.

GUI TOOL FOR PRE AND POST PROCESS

For quick and easy making of setting files and improvement of visibility of the result, the pre-post GUI (Grafic User Interface) tool of the MLZ model was developed, referring to CFD software on the market. Fig. 13 shows the flow of process for the prediction including the pre-post tool.
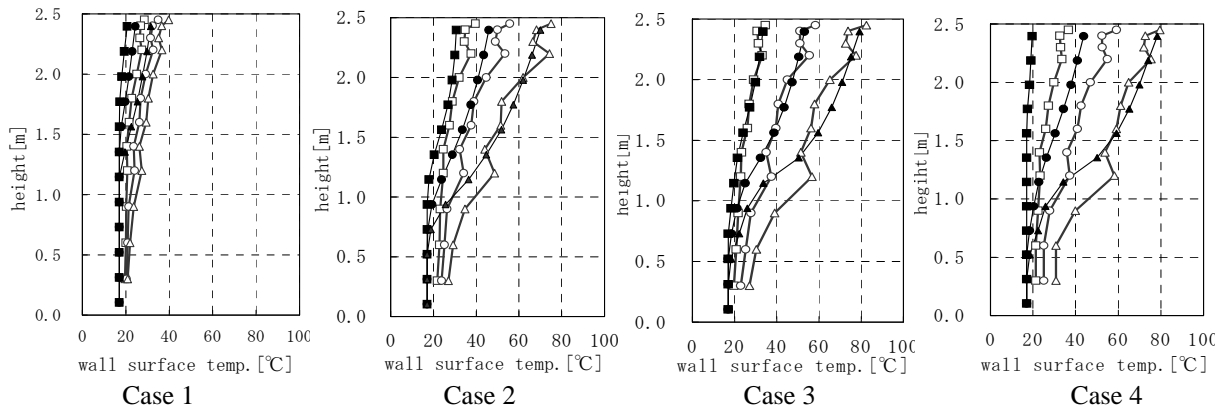

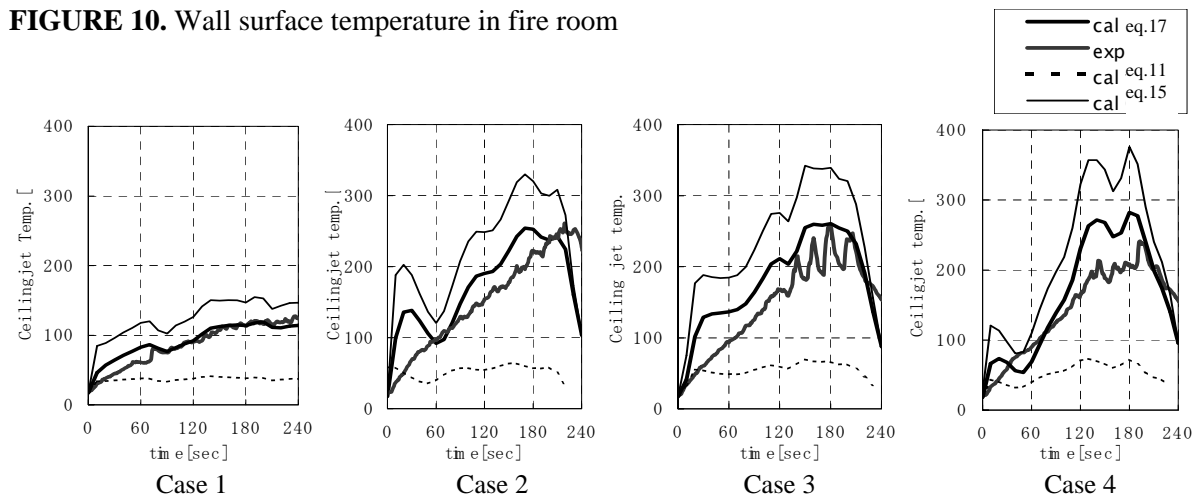**FIGURE 10.** Wall surface temperature in fire room

FIGURE 11. Gas temperature under ceiling in fire room
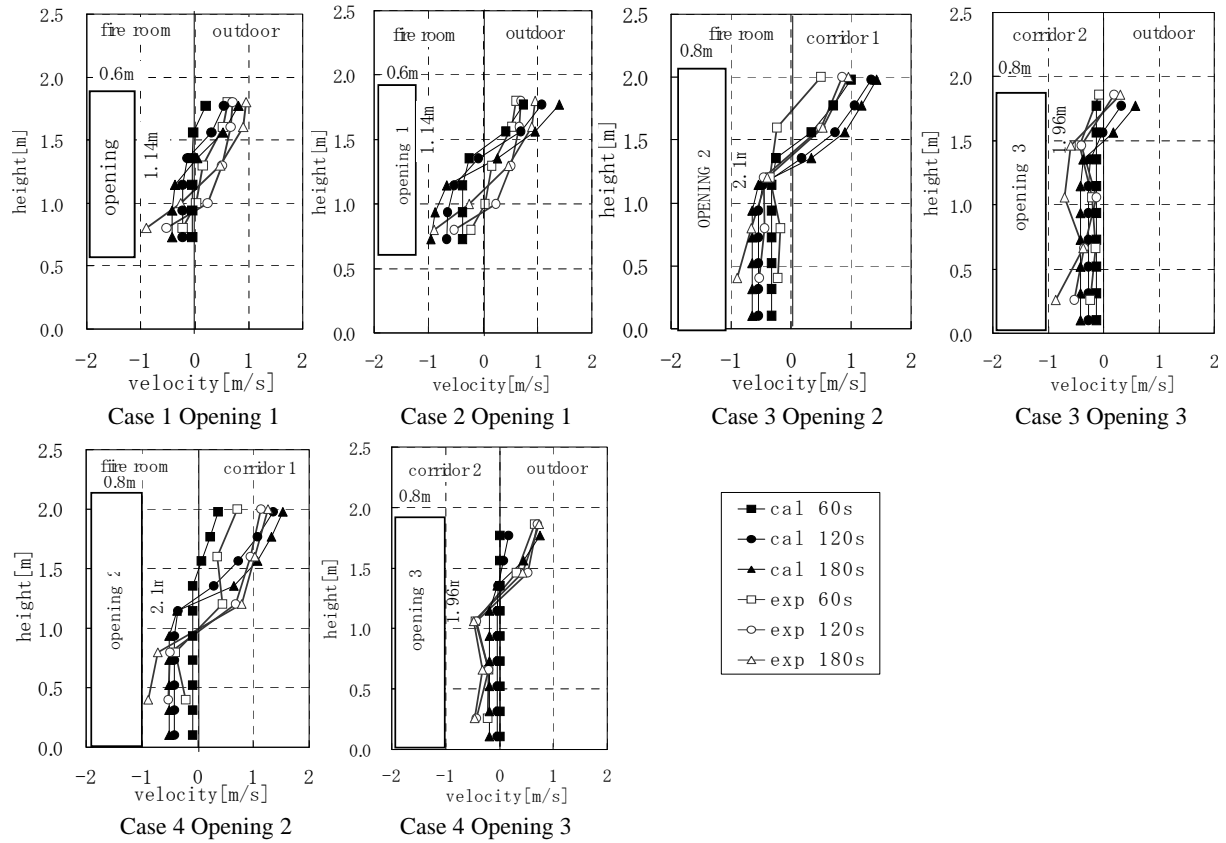
11

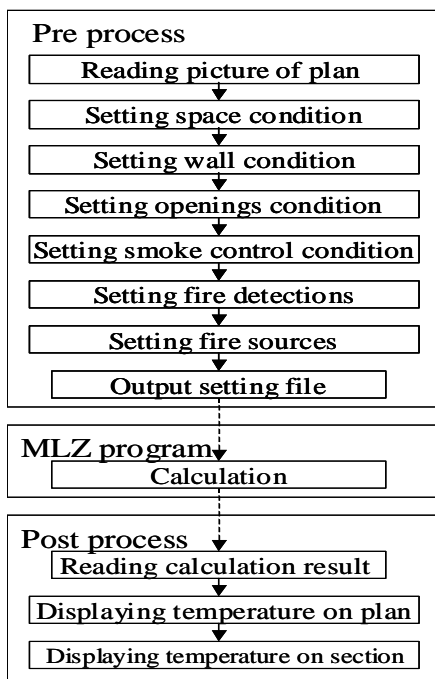**FIGURE 12.** Gas velocity through openings

FIGURE 13. Process of prediction

Firstly, the pre tool helps making a setting file. Boundaries of rooms are drawn by click and snap of mouse operation above an image file of a plane of an object space. Some other conditions such as the heat release rate of a fire source, an opening type, walls type can be set by selection from a pull-down box or by numeric input with key. Fig. 14 shows an image where input of a shape and some conditions of calculation area and a fire scenario was finished. As a supplement, the default values were inputted as a heat release rate and an exhaust gas flow rate in the standard fire safety design of Japan, and it is possible to plan comparatively early and quickly.

After the calculation of the MLZ program using the setting file, the post tool can display the calculation results visually. Fig. 15 shows an example of visualizing horizontal gas temperature data by color. Any height and any time can be selected or changed progressively like an animation. Fig. 16 shows a vertical distribution of gas temperature on a section, which is selected from any plane. In this version, only gas temperature and gas concentrations can be displayed by color.
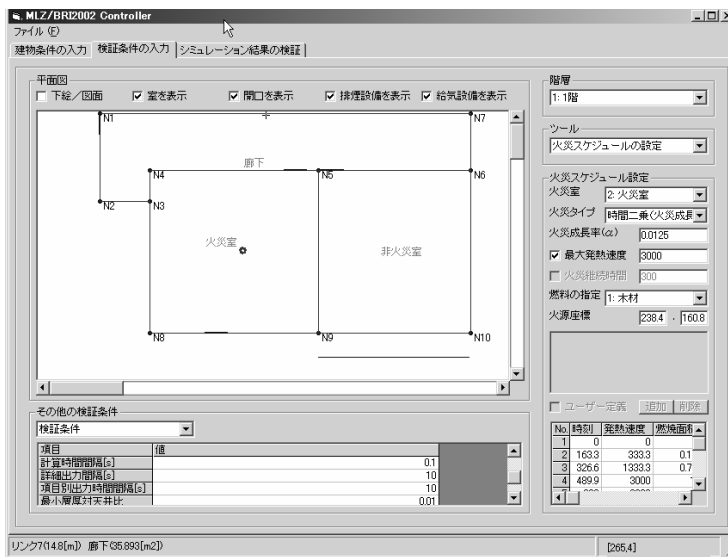

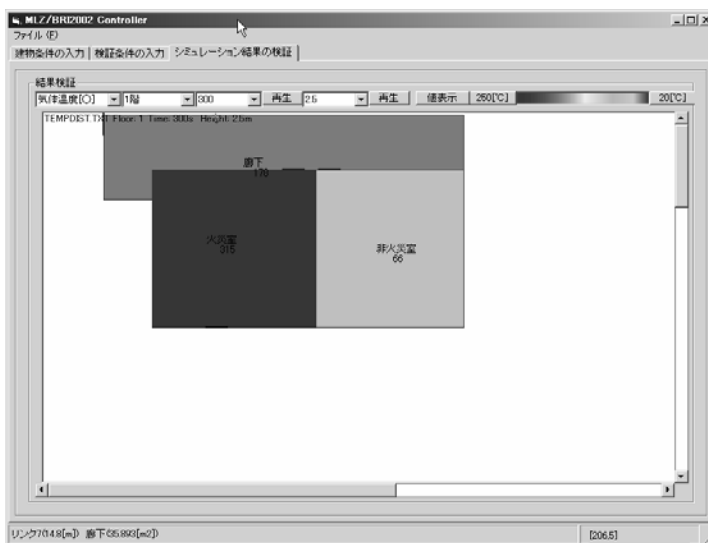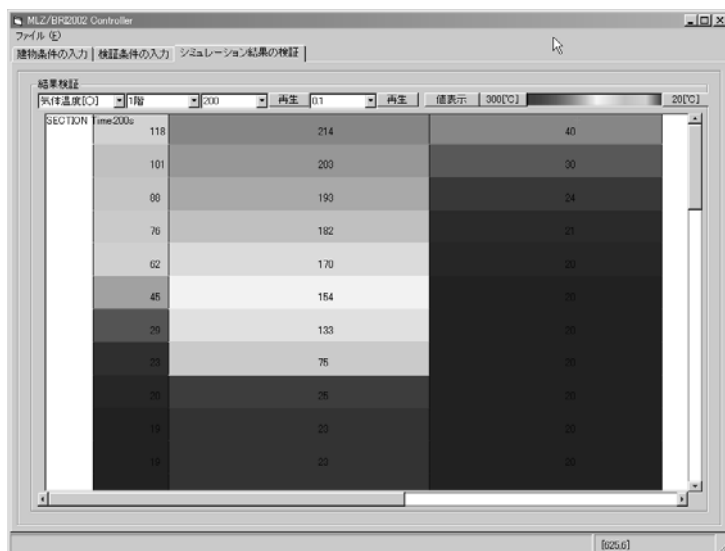**FIGURE 14.** Drawing the boundaries of rooms (pre)

FIGURE 15. Display of gas temperature on the plane (post)

FIGURE 16. Display of temperature distribution on the section (post)

CONCLUSION

In this study, the formulation of a MLZ model was extended to multi-room configuration, and also the refinements were made of the component models such as fire plume, opening jet plume, ceiling jet and radiation heat transfer. The validation was made against the full-scale fire experiment. Considerably satisfactory results were obtained from the validation, so the model present is considered to be a useful tool for fire protection design. However there is still room for further study on comparison with various experiments and confirmation of accuracy and applicability.

ACKNOWDGEMENT

REFERENCES

1. Tanaka, T. and Nakamura, K., "Model for Predicting Smoke Transport in Buildings - Base on Two Layer Zone Concept", Building Research Institute, No. 123, BRI, MOC, 1989.
2. K. Suzuki, K. Harada and T. Tanaka, "A Multi-Layer Zone Model for Predicting Fire Behavior in a Single room", The 7th Symposium of IAFSS, Jun, 2002.
3. Suzuki, K., Harada, K. Tanaka, T. and Yoshida, H., "An Application of a Multi-Layer Zone Model to a Tunnel Fire", 6th Asia-Oceania Symposium on Fire Science and Technology, 2004.
4. Zukoski, E.E., "Smoke Movement and Mixing in Two-Layer Fire Models", The 8th UJNR Joint Panel Meeting on Fire Research and Safety, Tsukuba, May, 1985.
5. J. G. Quintiere, "The Effect of Room Openings on Fire Plume Entrainment", Combustion Science and Technology, 1981.
6. Alpert, R.L., "Calculation of Response Time of Ceiling-Mounted Fire Detectors", Fire Technology, 1972.
7. Modak, A.T., "Radiation from Products of Combustion", Fire Research, 1, 1978/79.